Synthesis, Characterization, and Catalytic Properties of γ-Al_2O_3-Supported Zirconium Hydrides through a Combined Use of Surface Organometallic Chemistry and Periodic Calculations

Jérôme Joubert,[†] Françoise Delbecq,[†] Chloé Thieuleux,[‡] Mostafa Taoufik,[‡] Frédéric Blanc,[‡] Christophe Copéret,[‡] Jean Thivolle-Cazat,[‡] Jean-Marie Basset,*[,‡] and Philippe Sautet*[,†]

Laboratoire de Chimie, Institut de Chimie de Lyon, Université de Lyon, École Normale Supérieure de Lyon and CNRS, 46 Allée d'Italie, 69364 Lyon Cedex 07, France, and C2P2, Laboratoire de Chimie Organométallique de Surface (UMR 5265: CNRS-ESCPE Lyon), ESCPE Lyon, F-308, 43 Boulevard du 11 Novembre 1918, 69616 Villeurbanne Cedex, France

Received February 15, 2007

The treatment of the alumina-supported $[Zr(CH_2tBu)_4]$, $[(Al_sO)_2Zr(CH_2tBu)^+(tBuCH_2)Al_s^-]$, where Al_s stands for surface aluminum atoms, by H_2 yields a mixture of alumina-supported zirconium hydride species, $[(Al_sO)_2Zr(H)(\mu\text{-}H)Al_{VI}]$ and $[(Al_sO)_2Zr(H)(\mu\text{-}R)Al_{VI}]$, along with cationic $[(Al_sO)_2Zr(H)]^+$ in the vicinity of anionic tetrahedral aluminum hydrides $[Al_{IV}\text{-}H^-]$ according to mass balance analysis, reactivity studies, IR spectroscopy, and periodic calculations. Initial and final selectivities in the hydrogenolysis of alkanes as well as DFT calculations show that β-alkyl transfer is the key carbon−carbon cleavage step.

Introduction

Conversion of alkanes at low temperatures is still an important challenge today.[1,2] In 1990, it was shown for the first time that zirconium hydrides supported on silica[3−6] catalyze at low temperatures (e.g., 100−150 °C) the hydrogenolysis of alkanes with the exception of ethane.[7−9] Noteworthy, this reaction has been extended to the conversion of polyolefins, composed mainly of C−C σ-bonds, which are transformed into diesel range fuels and ultimately into methane/ethane mixtures.[10] This reaction was proposed to involve β-alkyl transfer as the key carbon−carbon bond cleavage step,[10−12] a step that corresponds to the microscopic reverse of the classical "Cossee" mechanism (insertion of an olefin into a M−C bond), the key step of the Ziegler−Natta polymerization. Depolymerization, forming olefins, is typically a highly endothermic process (eq 1), which requires high temperatures. Here, the use of H_2 displaces the thermodynamic equilibrium through the hydrogenation of the olefins (eq 2).

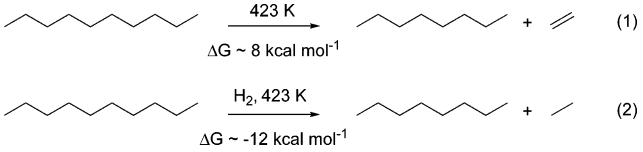

In the field of polymerization, it is known that alumina-supported organometallic complexes are usually more reactive than their corresponding silica equivalents,[13−20] and this has been "intuitively" associated with the presence of cationic species favored on "acidic" alumina and not on "neutral" silica. Recently we have shown that the reaction of $[Zr(CH_2tBu)_4]$ with alumina generates $[(Al_sO)_2Zr(CH_2tBu)^+(tBuCH_2)Al_s^-]$ (**1**), in which one of the neopentyl ligands has been transferred from Zr to an adjacent Al center, thus providing a true cationic species (surface aluminum atoms are noted Al_s). This readily explains the high reactivity of this system in the polymerization of olefines.[13−17,21]

We report here the synthesis, the characterization, and the mechanism of formation of the alumina-supported zirconium hydrides prepared by treatment with H_2 of $[(Al_sO)_2Zr(CH_2tBu)^+(tBuCH_2)Al_s^-]$ (**1**). Moreover, we have also investigated its

* Corresponding author. E-mail: philippe.sautet@ens-lyon.fr.
[†] École Normale Supérieure de Lyon and CNRS.
[‡] UMR 5265: CNRS-ESCPE Lyon.

(1) Crabtree, R. H. *J. Chem. Soc., Dalton Trans.* **2001**, 2437−2450.
(2) Labinger, J. A.; Bercaw, J. E. *Nature* **2002**, *417*, 507−514.
(3) Zakharov, V. A.; Dudchenko, V. K.; Paukstis, E.; Karakchiev, L. G.; Ermakov, Y. I. *J. Mol. Catal.* **1977**, *2*, 421−435.
(4) Zakharov, V. A.; Ryndin, Y. A. *J. Mol. Catal.* **1989**, *56*, 183−193.
(5) Yermakov, Y. I.; Ryndin, Y. A.; Alekseev, O. S.; Kochubei, D. I.; Shmachkov, V. A.; Gergert, N. I. *J. Mol. Catal.* **1989**, *49*, 121−132.
(6) Corker, J.; Lefebvre, F.; Lecuyer, C.; Dufaud, V.; Quignard, F.; Choplin, A.; Evans, J.; Basset, J.-M. *Science* **1996**, *271*, 966−969.
(7) Lécuyer, C.; Quignard, F.; Choplin, A.; Olivier, D.; Basset, J. M. *Angew. Chem., Int. Ed. Engl.* **1991**, *30*, 1660−1661.
(8) Thieuleux, C.; Copéret, C.; Dufaud, V.; Marangelli, C.; Kuntz, E.; Basset, J. M. *J. Mol. Catal. A* **2004**, *213*, 47−57.
(9) Copéret, C.; Candy, J. P.; Basset, J. M. *Top. Organomet. Chem.* **2005**, *16*, 151.
(10) Dufaud, V.; Basset, J. M. *Angew. Chem., Int. Ed.* **1998**, *37*, 806−810.
(11) Mortensen, J. J.; Parrinello, M. *J. Phys. Chem. B* **2000**, *104*, 2901−2907.
(12) Besedin, D. V.; Ustynyuk, L. Y.; Ustynyuk, Y. A.; Lunin, V. V. *Mendeleev Commun.* **2002**, 173−175.
(13) Ballard, D. G. H. *Coord. Polym.* **1975**, 223−262.
(14) Ballard, D. G. H. *J. Polym. Sci. Polym. Chem. Ed.* **1975**, *13*, 2191−2212.
(15) Tullock, C. W.; Tebbe, F. N.; Mulhaupt, R.; Ovenall, D. W.; Setterquist, R. A.; Ittel, S. D. *J. Polym. Sci. A* **1989**, *27*, 3063−3081.
(16) Collette, J. W.; Tullock, C. W.; MacDonald, R. N.; Buck, W. H.; Su, A. C. L.; Harrell, J. R.; Mulhaupt, R.; Anderson, B. C. *Macromolecules* **1989**, *22*, 3851−3858.
(17) Tullock, C. W.; Mulhaupt, R.; Ittel, S. D. *Makromol. Chem., Rapid Commun.* **1989**, *10*, 19−23.
(18) Marks, T. J. *Acc. Chem. Res.* **1992**, *25*, 57−65.
(19) Jezequel, M.; Dufaud, V.; Ruiz-Garcia, M. J.; Carrillo-Hermosilla, F.; Neugebauer, U.; Niccolai, G. P.; Lefebvre, F.; Bayard, F.; Corker, J.; Fiddy, S.; Evans, J.; Broyer, J.-P.; Malinge, J.; Basset, J.-M. *J. Am. Chem. Soc.* **2001**, *123*, 3520−3540.
(20) Copéret, C.; Chabanas, M.; Petroff Saint-Arroman, R.; Basset, J.-M. *Angew. Chem., Int. Ed.* **2003**, *42*, 156−181.
(21) Joubert, J.; Delbecq, F.; Sautet, P.; Le Roux, E.; Taoufik, M.; Thieuleux, C.; Blanc, F.; Copéret, C.; Thivolle-Cazat, J.; Basset, J.-M. *J. Am. Chem. Soc.* **2006**, *128*, 9157−9169.

10.1021/om070145f CCC: $37.00
Publication on Web 06/08/2007

hydrogenolysis properties. All these studies have been achieved through a combined use of experimental and theoretical approaches.

Experimental Section

General Procedure. All experiments were conducted under strict inert atmosphere or vacuum conditions using standard Schlenk techniques. Solvents were purified and dried according to standard procedures. Alkanes and H_2 were dried over freshly regenerated molecular sieves (3 Å) and deoxo traps before addition. $[Zr(CH_2tBu)_4]$ was purchased from Aldrich and sublimed prior to use. γ-$Al_2O_{3-(500)}$ was purchased from Degussa (C Aerosil). Elemental analyses were performed at the CNRS Central Analysis Service of Solaize (Zr) and at the University of Bourgogne (C). Gas-phase (GC) analysis of alkanes was performed on a Hewlett-Packard 5890 series II gas chromatograph equipped with a flame ionization detector and a KCl/Al_2O_3 on a fused silica column (50 m × 0.32 mm). Hydrogen was analyzed using a Intersmat-IGC 120-MB gas chromatograph equipped with a molecular sieves column and a catharometer. Infrared spectra were recorded on a Nicolet 550-FT by using an infrared cell equipped with CaF_2 windows, allowing *in situ* studies. Typically 16 scans were accumulated for each spectrum (resolution, 2 cm^{-1}).

Preparation of Partially Dehydroxylated Alumina at 500 °C, $Al_2O_{3-(500)}$. γ-Al_2O_3 was calcined at 500 °C under N_2/O_2 flow overnight and then partially dehydroxylated at 500 °C under high vacuum (0.13 mPa) for 12−24 h to give a white solid. The specific surface area of γ-$Al_2O_{3-(500)}$ as measured by BET was 90 m^2/g, and the OH density was 4.0 OH/nm^2 (0.6 mmol/g). ^{27}Al CP MAS NMR: δ_{Al} 4 (3 Al, Oh), 62 ppm (1 Al, Td).

Monitoring the Grafting of $Zr(CH_2tBu)_4$ on Alumina and the Subsequent Treatment under H_2 by IR Spectroscopy. Representative Procedure. γ-Al_2O_3 (100 mg) was pressed into an 18 mm self-supporting disk, adjusted in the sample holder, and put into a glass reactor equipped with CaF_2 windows. The support was prepared as described above, and $[Zr(CH_2tBu)_4]$ was then sublimed under high vacuum (1.34 Pa) at 80 °C onto the alumina disk. The solid was then heated at 65 °C for 2 h before the excess of complexes was removed by reverse sublimation at 80 °C and condensed into a tube cooled with liquid N_2, which was then sealed off using a torch to yield **1**. A large excess of anhydrous H_2 (77 330 Pa) was introduced in the IR cell, which was then heated at 150 °C. After 15 h, the gaseous product was quantified by GC. An IR spectrum was recorded at each step.

Preparation of Alumina-Supported Zirconium Hydrides on Larger Quantities. Representative Procedure. The surface species **1** (165 mg, 24 μmol of Zr, 1 equiv), prepared according to the reported procedure, was loaded in a Schlenk tube in a glovebox.[21] After evacuation of Ar, a large excess of anhydrous H_2 (77 330 Pa, 13.5 mmol) was introduced, and the reaction mixture heated at 150 °C for 15 h. The color turned from white to beige, and the gaseous products (methane and ethane) were quantified by GC with the following composition: methane (138 μmol, 5.6 equiv/Zr) and ethane (47 μmol, 1.9 equiv/Zr).

Hydrolysis of Alumina-Supported Zirconium Hydrides. Representative Procedure. In a 39 mL reactor, an excess of H_2O vapor (5 333 Pa, 86 μmol, 5 equiv/Zr) was condensed onto the alumina-supported zirconium hydrides (96 mg, 16.9 μmol of Zr, 1 equiv) cooled at −196 °C. The reaction mixture was warmed to 25 °C and stirred forr 12 h, and the gaseous products were quantified by GC: H_2 (24 ± 4 μmol, 1.4 ± 0.2 equiv/Zr), methane (2.8 μmol, 0.16 equiv/Zr), ethane (0.4 μmol, 0.02 equiv/Zr), propane (0.2 μmol, 0.01 equiv/Zr), butane (0.6 μmol, 0.03 equiv/Zr), 2,2-dimethylpropane (8.0 μmol, 0.50 equiv/Zr), pentane (0.1 μmol, 0.002 equiv/Zr).

Hydrogenolysis of Butane with Alumina-Supported Zirconium Hydrides. A mixture of alumina-supported zirconium hydrides (107 mg, 18.8 μmol of Zr, 1 equiv), butane (5 900 Pa, 0.80 mmol, 44 equiv), and H_2 (95 700 Pa, 13.3 mmol, 705 equiv) in a Pyrex-glass batch reactor (370 mL) was heated with an oil bath at 160 ± 1 °C. During the reaction, aliquots were expended in a small volume, brought to atmospheric pressure, and analyzed by GC.

Computational Details

The calculations were performed within the framework of density functional theory (DFT) using a periodic description of the system as implemented in the VASP code.[22,23] The generalized gradient approximation was used in the formulation of Perdew and Wang PW91.[24] Atomic cores are described with the projected augmented wave method (PAW), which is equivalent to an all-electron frozen core approach.[25,26] The one-electron wave functions are developed on a basis set of plane waves. With the selected PAW potentials, a cutoff energy of 275 eV is adequate and yields a converged total energy: a 1 meV/atom mean variation occurs when varying the cutoff energy from 275 eV up to 400 eV.

The Brillouin zone integration is converged with a 331 k-point mesh generated by the Monkhorst−Pack algorithm.[27] The vibrational frequencies are calculated in the harmonic approximation by a numerical evaluation of the Hessian matrix. With such a description of the system, one can expect an evaluation of energetics within a precision below 15 kJ·mol^{-1}.[28] The (110) surface of γ-alumina is the most exposed one in particles (75%) and is described here by a four-layer periodic slab of unit formula $Al_{16}O_{24}$ with cell vectors of 8.4 × 8.1 $Å^2$.

The surface has been modeled by a periodic slab, and the various envisaged adsorptions have been performed on only one face of the slab, generating an asymmetric surface representation. The thickness of the model slab has been sampled from eight to four atomic layers with no significant changes. Thus, a four-layer slab has been used as a standard model. With such an asymmetric representation of the surface, some dipole correction may be necessary. Tests reveal only infinitesimal changes in geometries, and the energetic corrections are below 5 kJ·mol^{-1}, which is coherent with the large vacuum zone between the slabs (∼17 Å). Thus, such corrections have not been applied. In realistic conditions the alumina surface is hydroxylated. The simulation of IR spectra shows that the trihydrated surface unit cell with a OH coverage of 8.8 OH/nm^2 (versus 4 OH/nm^2 determined experimentally for the total alumina surface) correctly describes the diversity of OH groups present on γ-Al_2O_3 pretreated at 500 °C.[21,29−33] OH groups interact with one, two, or three Al atoms, while the surface aluminum atoms have a coordination ranging from IV to VI and interact with one or two OH groups. In addition, it was shown from both experiment

(22) Kresse, G.; Furthmueller, J. *Comput. Mater. Sci.* **1996**, *6*, 15−50.
(23) Kresse, G.; Furthmueller, J. *Phys. Rev. B* **1996**, *54*, 11169−11186.
(24) Perdew, J. P.; Chevary, J. A.; Vosko, S. H.; Jackson, K. A.; Pederson, M. R.; Singh, D. J.; Fiolhais, C. *Phys. Rev. B* **1992**, *46*, 6671−6687.
(25) Bloechl, P. E. *Phys. Rev. B* **1994**, *50*, 17953−17979.
(26) Bloechl, P. E.; Forst, C. J.; Schimpl, J. *Bull. Mater. Sci.* **2003**, *26*, 33−41.
(27) Monkhorst, H. J.; Pack, J. D. *Phys. Rev. B* **1976**, *13*, 5188.
(28) Lynch, B. J.; Truhlar, D. G. *J. Phys. Chem. B* **2001**, *105*, 2936−2941.
(29) Digne, M.; Sautet, P.; Raybaud, P.; Euzen, P.; Toulhoat, H. *J. Catal.* **2002**, *211*, 1−5.
(30) Digne, M.; Sautet, P.; Raybaud, P.; Toulhoat, H.; Artacho, E. *J. Phys. Chem. B* **2002**, *106*, 5155−5162.
(31) Digne, M.; Sautet, P.; Raybaud, P.; Euzen, P.; Toulhoat, H. *J. Catal.* **2004**, *226*, 54−68.
(32) Joubert, J.; Salameh, A.; Krakoviack, V.; Delbecq, F.; Sautet, P.; Copéret, C.; Basset, J. M. *J. Phys. Chem. B* **2006**, *110*, 23944−23950.
(33) Joubert, J.; Fleurat-Lessard, P.; Delbecq, F.; Sautet, P. *J. Phys. Chem. B* **2006**, *110*, 7392−7395.

Scheme 1. Proposed Surface Species Based on Experimental Data

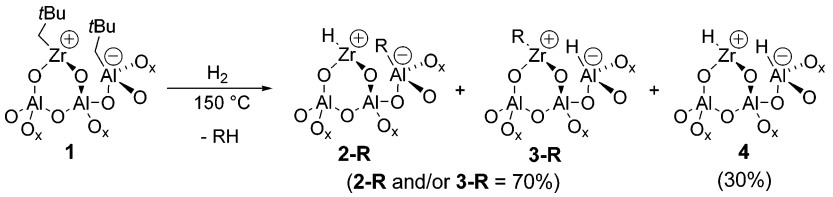

and theory that the hydration of alumina is not uniform, with the presence of hydration defects.[32,34]

Results and Discussion

Synthesis and Characterization of Alumina-Supported Zirconium Hydrides. Monitoring by IR Spectroscopy. As previously described,[21] the reaction of an excess of $[Zr(CH_2tBu)_4]$ on an alumina disk partially dehydroxylated at 500 °C ($Al_2O_{3-(500)}$) generates the cationic Zr surface complex $[(Al_sO)_2Zr(CH_2tBu)^+(tBuCH_2)Al_s^-]$ (**1**) as the major surface species. This species displays the characteristic IR bands in the 3000−2700 and 1500−1300 cm^{-1} regions associated with the $\nu_{(CH)}$ and $\delta_{(CH)}$ of the remaining perhydrocarbyl ligands attached to Zr and Al. After treatment at 150 °C under a large excess of H_2, these peaks have clearly decreased in intensity, and two main signals have appeared at 1919 and 1622 cm^{-1}, consistent with Al−H[35] and Zr−H,[5,6,36,37] respectively.

Concomitantly, methane and ethane are formed in a 3:1 ratio, and they result from the hydrogenolysis of the neopentyl ligands (typically present as 2.3 ± 0.2 equiv/Zr in $[Zr(CH_2tBu)_4/\gamma\text{-}Al_2O_{3-(500)}]$; 2.0 expected for structure **1**). The ethane-to-methane ratio is the same as that observed during the hydrogenolysis of the well-defined silica-supported trisneopentyl zirconium complex $[(\equiv SiO)Zr(CH_2tBu)_3]$ carried out under similar reaction conditions.[7] This 3-to-1 methane/ethane ratio and the stability of ethane under hydrogenolysis conditions for the silica-supported systems have been interpreted as evidence for β-alkyl transfer being the key carbon−carbon cleavage step.[7−9] Indeed, this mechanism requires having a C−C bond in the β-position with respect to the metal, the successive cleavage of a neopentyl species leading to three methane molecules. The formed Zr-ethyl intermediate can then only undergo hydrogenolysis of the M−C bond to generate one ethane. It is therefore likely that the mechanism of carbon−carbon cleavage for the alumina-supported zirconium hydrides is similar (*vide infra* for further comments). During the treatment of **1** under H_2, the total amount of carbons formed corresponds to the hydrogenolysis of ca. 1.6 ± 0.3 equiv of neopentyl ligands, which shows that some residual alkyl ligands must be present at the surface {expected = (2.3 − 1.6) = 0.7 equiv}.[21] In fact, upon hydrolysis,[20] 1.3 ± 0.2 H_2 per Zr is evolved along with 0.7 equiv of alkanes, mainly as methane (0.16 equiv) and 2,2-dimethylpropane (0.5 equiv). These alkanes arise from the hydrolysis of residual M-alkyl species, not hydrogenolyzed under H_2. Such a phenomenon has already been observed during the preparation of oxide-supported hydrides.[37] Overall, the alumina-supported zirconium hydrides contain 1.3 hydride and 0.7 alkyl ligand per Zr, and this system can be formulated as a mixture of (alkyl)(hydrido) species (70%), leading to 0.7 H_2 and 0.7 alkane per Zr upon hydrolysis, and of a bishydride species (30%), leading to 0.6 H_2. On the basis of the structure of **1**, these species can be tentatively described as $\{[(Al_sO)_2Zr(H)^+](R-Al_s^-)]$ (**2-R**), $\{[(Al_sO)_2Zr(-R)]^+(H-Al_s^-)\}$ (**3-R**), and $\{[(Al_sO)_2Zr(H)]^+(H-Al_s^-)\}$ (**4**) (Scheme 1, *vide infra* for further comments).

Periodic Calculations. The alumina-supported neopentylzirconium complex has been previously studied from DFT calculations both with model ligands (CH_3) and with the full ligand sets (neopentyl).[21] From the exploration of the energy profile of the grafting reaction, and by comparison with experimental data, it was shown that the surface species is mainly a bisaluminoxy cationic complex, with one alkyl ligand remaining on the Zr atom and the other one partially transferred onto an adjacent surface Al Lewis acid site. The model ligand CH_3 has been selected to further investigate the formation of the alumina-supported zirconium hydride grafted complex from $\{(Al_sO)_2Zr(R)^+(\mu\text{-}R)(Al_s)^-\}$ (R = CH_3, **1m**, Scheme 2 and Figure 2). The calculated structure of all surface species **1**, **2**, etc. will be noted as **1m**, **2m**, etc.

The alkane release can occur via hydrogenolysis of the Zr−C bond through σ-bond metathesis. In **1m**, there are one terminal and one bridging CH_3 between the Zr and one Al atom. Hydrogenolysis of the terminal methyl in **1m** giving **2m-Me** is associated with a relatively low activation energy ($\Delta E^{\ddagger} = 60$ kJ·mol^{-1}) and is exoenergetic ($\Delta E = -32$ kJ·mol^{-1}). In contrast, hydrogenolysis of the bridging methyl giving **3m-Me**, although being more exoenergetic ($\Delta E = -62$ kJ·mol^{-1}), is far more difficult ($\Delta E^{\ddagger} \approx 160$ kJ·mol^{-1}). This bridging methyl is probably less reactive because it is more located on the aluminum atom, as evidenced by the long Zr−C (2.77 Å) and the relatively short Al−C (2.07 Å) distances.

From **2m-Me**, hydrogenolysis of the μ-CH_3 via σ-bond metathesis gives the bishydride **4m** with one bridging hydride between Zr and Al (Figures 2 and 3). This reaction is exoenergetic ($\Delta E = -60$ kJ·mol^{-1}), and the associated activation energy is lower than for the hydrogenolysis of μ-CH_3 in **1m**: $\Delta E^{\ddagger} = 108$ kJ·mol^{-1} (vs 160 kJ·mol^{-1}). The origin of the large difference between the two activation energies for the two hydrogenolysis transition states can be explained as follows (Scheme 2): $TS_{\mathbf{1m\rightarrow 2m}}$ is a classical transition state for a σ-bond metathesis with the alignment of H−H−CH_3 coordinated to the Zr atom, while, in $TS_{\mathbf{1m\rightarrow 3m}}$, the μ-CH_3 ligand cannot approach the Zr atom due to the presence of the ancillary CH_3 ligand (it is an hydride in $TS_{\mathbf{2m\rightarrow 4m}}$). Thus, the formation of the C−H bond has to occur without the assistance of the Zr atom, and methane is almost completely formed in the transition state. The relaxation of the structure is due to only the bond angles' adjustment after the formation of the C−H and Zr−H bonds.

Because the barrier for the hydrogenolysis of the Zr−CH_3 bond in **2m-Me** (σ-bond metathesis) is still rather high, we also investigated other reaction pathways. The model complex **2m-Me** can isomerize in the neutral intermediate **5m-Me** $\{(Al_sO)_2$-

(34) Métivier, R.; Leray, I.; Roy-Auberger, M.; Zanier-Szydlowski, N.; Valeur, B. *New J. Chem.* **2002**, *26*, 411−415.
(35) Dunken, H.; Fink, P. *Z. Chem.* **1966**, *6*, 194−195.
(36) Quignard, F.; Lecuyer, C.; Choplin, A.; Olivier, D.; Basset, J. M. *J. Mol. Catal.* **1992**, *74*, 353−363.
(37) Rataboul, F.; Baudouin, A.; Thieuleux, C.; Veyre, L.; Copéret, C.; Thivolle-Cazat, J.; Basset, J.-M.; Lesage, A.; Emsley, L. *J. Am. Chem. Soc.* **2004**, *126*, 12541−12550.

Scheme 2. Cationic Alkyl-Zirconium Model Complex (1m) Precursor to the Alumina-Supported Zirconium Hydrides 2m-Me, 3m-Me, 4m-Me, 5m-Me, and 6m

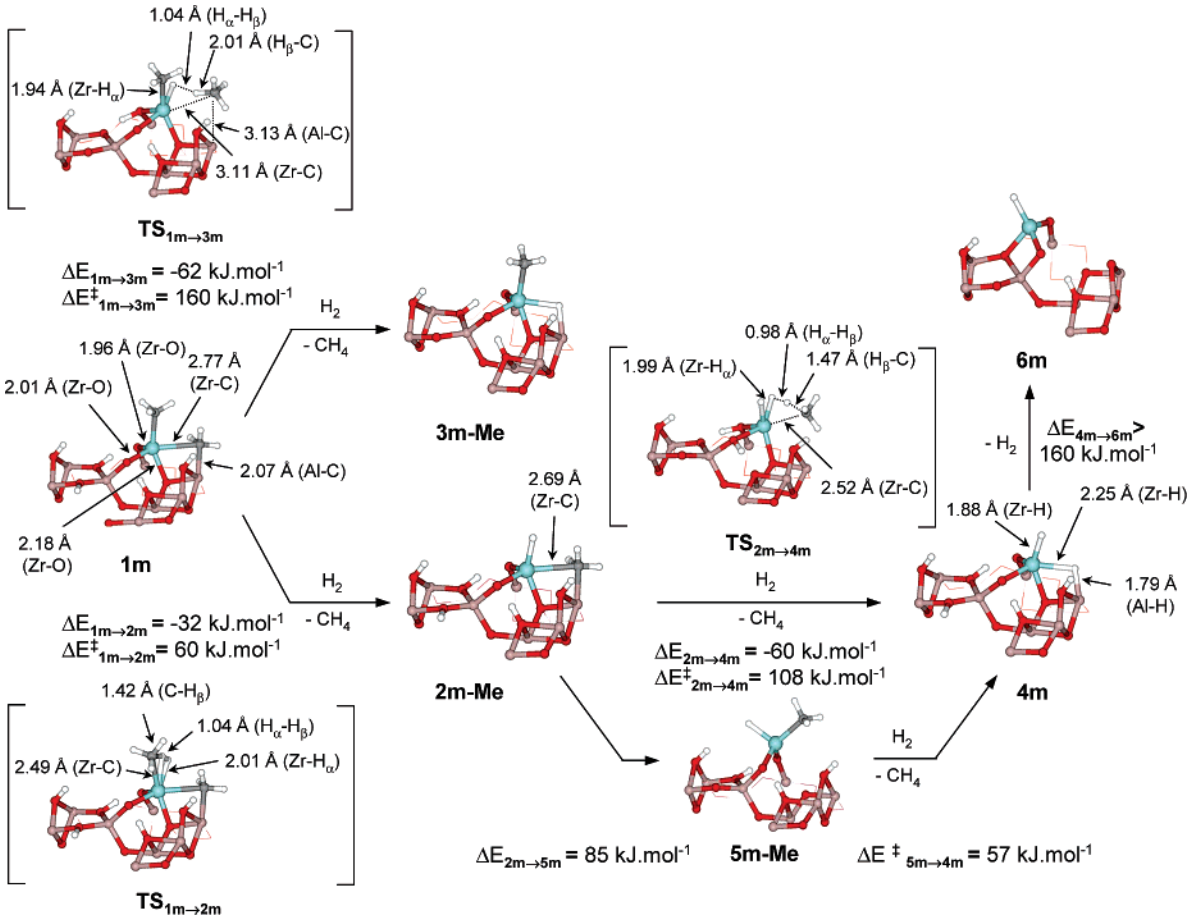

Zr(H)(CH_3)} prior to hydrogenolysis. This reaction is endoenergetic ($\Delta E = 85$ kJ·mol^{-1}), and the associated activation barrier of this reaction is probably close to the energeticity of the reaction because the corresponding reverse reaction, i.e., transfer of terminal methyl onto an Al center to form partially cationic species, has already been shown to be exoenergetic and weakly activated (<5 kJ·mol^{-1}).[21] Hydrogenolysis of the Zr−C bond in **5m-Me** via σ-bond metathesis has a low activation barrier, 57 kJ·mol^{-1}, but overall the reaction from **2m-Me** to **4m** via **5m-Me** is far more activated (142 kJ·mol^{-1}) compared to the direct pathway (108 kJ·mol^{-1}) as shown in Figure 2. In fact, a kinetic model based on Eyring theory shows that the one-step process would occur 10^5 times faster than the two-step process. The formation of the monohydride **6m** from **4m** by H_2 desorption has also been tested, but this reaction is endoenergetic by more than 120 kJ·mol^{-1}.

Overall, the calculations are in agreement with experimental chemical reactivity data: the treatment of **1** with H_2 can yield Zr species, having two remaining ligands (H or R), like **4** and **2-R**, while a monohydride complex **6** cannot be formed. Moreover, the calculations also show that the formation of **4m** via the hydrogenolysis of the bridging methyl ligand in **2m-Me** is the rate-limiting step, and this is consistent with the presence of both **4** and **2-R** after treatment of **1** with H_2, **3-R** being less likely because it is less easily obtained from **1** and more easily hydrogenolyzed than either **4** or **2-R**.

Evidence for **4** has been further investigated by calculating the infrared spectrum of the bishydride model surface complex {$(Al_sO)_2$Zr(H)(μ-H)Al_{VI}} (**4m**). The terminal Zr−H stretching frequency has been calculated at 1620 cm^{-1}, in agreement with the experimental data (1622 cm^{-1}), and the Zr−(μ-H)−Al_{VI} stretching frequency (which is more an Al−H than a Zr−H stretching according to the metal−hydride distances) has been calculated to be 1410 cm^{-1}, which can correspond to the weak band observed at 1415 cm^{-1}. Note that, in both cases, the agreement with experimental data is beyond the expected 20 cm^{-1} error bar for the DFT-PW91-calculated frequencies.

These results do not explain the observed band at 1919 cm^{-1}, and further improvement of the model is needed. We showed in our previous work that the calculated stretching frequency of a hydride on a tetrahedral aluminum atom is 1920 cm^{-1}.[32] Thus the experimental band at 1919 cm^{-1} can be attributed to these surface species. We have shown previously (see ref 21 for more details) that the grafting of ZrR_4 complexes on alumina also leads to the formation of cationic complexes [$(Al_sO)_2$Zr−R]$^+$ in the vicinity of anionic [(Al_{IV}−R)$^-$] species, the Al being tetrahedral (it is octahedral in **1m**). Hydration defects on the alumina surface are required to form these species.[32] Their hydrogenolysis probably produces the observed tetrahedral aluminum hydride [(Al_{IV}−H)$^-$] in the vicinity of a cationic [$(Al_sO)_2$Zr−H]$^+$. Formation of Al_{IV}−H species could also be possible by an exchange between the μ-H of **4m** with a tetrahedral aluminum hydroxyl, but while this process is exoenergetic ($\Delta E = -20$ kJ·mol^{-1}), no pathway with reasonable barrier has been found for the migration of anionic species (H$^-$ or OH$^-$) on the alumina surface, which excludes this exchange.

Hydrogenolysis of Butane with Alumina-Supported Zirconium Hydrides. During the formation of the alumina-supported zirconium hydrides, a 3:1 methane-to-ethane ratio has been observed due to the hydrogenolysis of alkyl ligands on

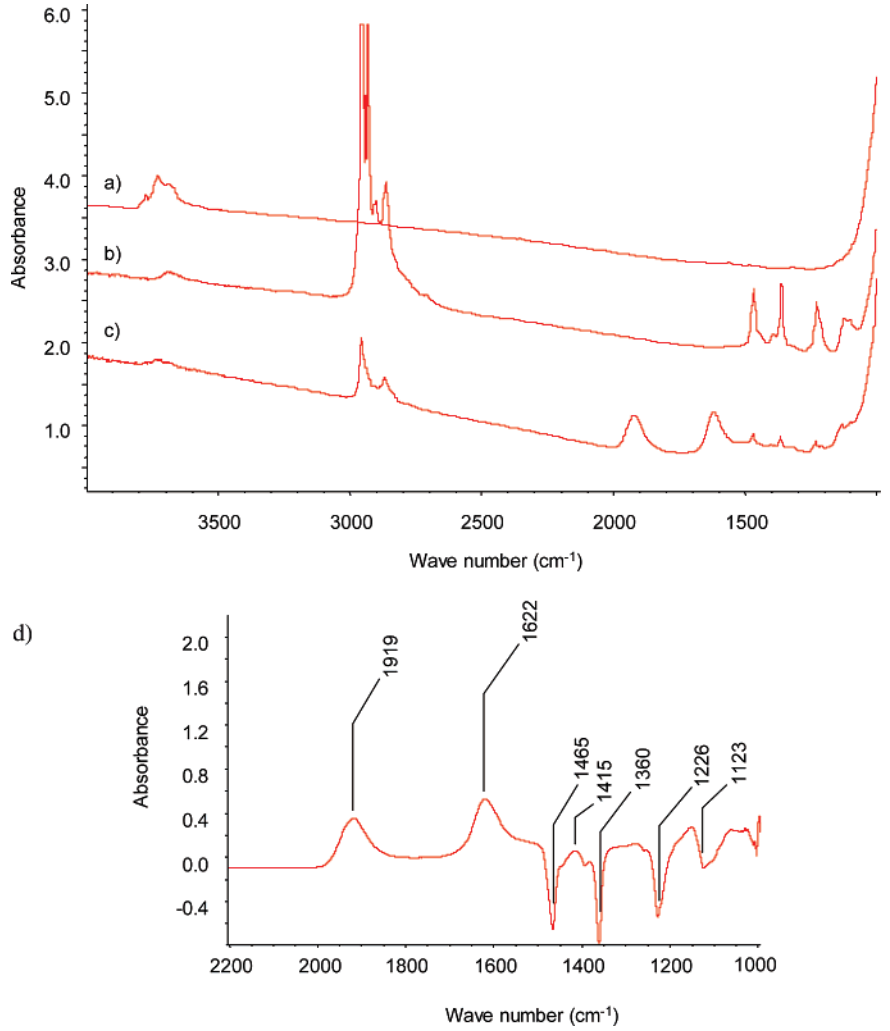

Figure 1. IR spectra of (a) γ-Al_2O_3 calcined and treated under vacuum at 500 °C, γ-$Al_2O_{3-(500)}$, (b) γ-$Al_2O_{3-(500)}$ after reaction at 70 °C with $Zr(CH_2tBu)_4$, [$Zr(CH_2tBu)_4/\gamma$-$Al_2O_{3-(500)}$], and (c) after treatment of [$Zr(CH_2tBu)_4/\gamma$-$Al_2O_{3-(500)}$] with H_2 for 15 h at 150 °C and (d) subtracted spectrum (c − b).

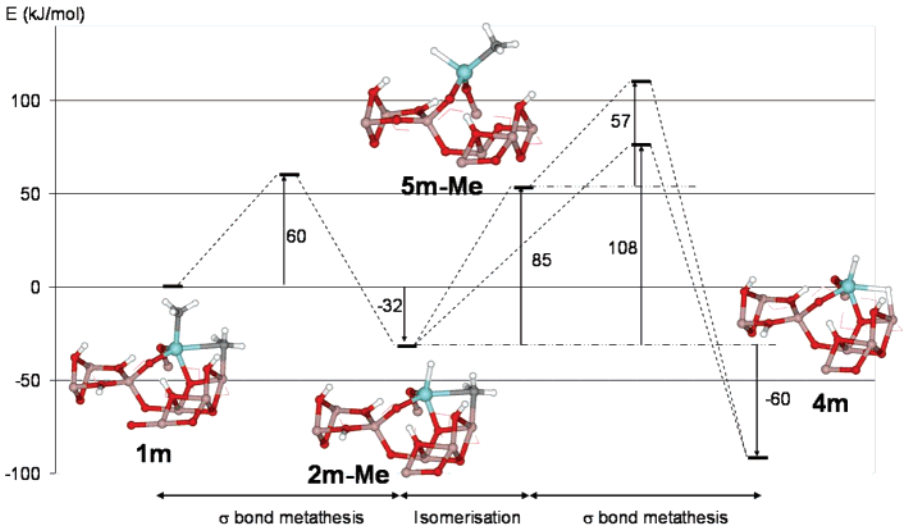

Figure 2. Reaction path for the formation of {$(Al_sO)_2Zr(H)(\mu$-$H)Al_s$}(**4m**).

the newly formed zirconium hydride. We have therefore investigated this hydrogenolysis mechanism through the use of a model alkane, e.g., butane, and modeled the reaction path by periodic calculations.

Experimental Data. Alumina-supported zirconium hydrides catalyze the hydrogenolysis of butane with an initial turnover frequency of 113 TON/h. The initial selectivities in methane, ethane, propane, and isobutane at low conversions are 24, 54, 19, and 3%, respectively. As the reaction proceeds, propane is transformed into methane and ethane, and the final composition

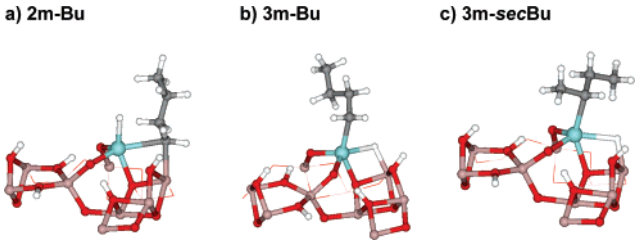

Figure 3. Optimized geometries of butylzirconium surface complexes resulting from reaction of **4m** and the primary C−H bond of butane.

Scheme 3. Selectivity in Primary Product for an Alkane Hydrogenolysis through β-Alkyl Transfer as a Key Carbon−Carbon Bond Cleavage Step

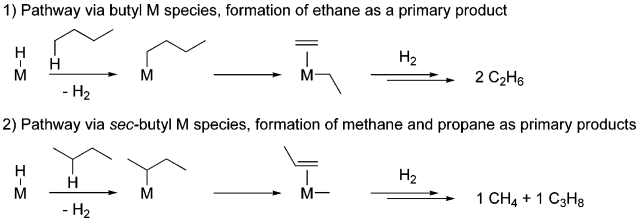

of the reaction mixture is a 3-to-2 mixture of ethane and methane. All these data (initial rates, initial and final selectivities) are similar to those obtained for the silica-supported zirconium hydrides,[7−9] which can be the sign of a similar mechanism. While methane and propane result from the hydrogenolysis of the *sec*-butyl zirconium species, ethane (as a primary product) arises from the hydrogenolysis of the butyl zirconium species (Scheme 3). Considering the difference of selectivities at 150 °C between the two pathways (54% butyl vs 46% *sec*-butyl, calculated from initial selectivity), one can conclude that these hydrogenolysis pathways are probably very similar.

Investigation of the Hydrogenolysis Reaction Mechanism by Periodic Calculations. Using **4m** $[(Al_sO)_2Zr(H)(\mu\text{-}H)Al_s]$ as a model for alumina-supported zirconium hydrides, we have investigated the reaction pathway of the hydrogenolysis of butane. The first step is the C−H activation of butane via σ-bond metathesis. This is the only possible pathway because Zr is in its highest stable oxidation state, which precludes oxidative-addition as a possible elementary step, and the direct σ-bond metathesis between Zr−H and C−C has not been investigated because it has been shown that having a carbon atom in the β-position of a σ-bond metathesis transition state always results in a high activation energy (>240 kJ·mol^{-1}).[38,39]

Thus, σ-bond metathesis between Zr−H and C−H bonds has been tested. Four pathways and intermediate alkyl complexes are possible, whether butane is activated through its primary or secondary C−H bond, and whether the C−H bond activation occurs at the terminal or the bridging hydride of **4m** (Scheme 4).

Activation of the terminal C−H bonds of butane on **4m** leads to the formation of **2m-Bu** and **3m-Bu** (Figure 3a,b). The latter is endoenergetic by 45 kJ·mol^{-1}, while the former is even more endoenergetic (99 kJ·mol^{-1}). Moreover, because the corresponding reaction of methane shows that σ-bond metathesis processes involving the bridging hydride are more activated (*vide supra*, Figure 3), the kinetics of the C−H bond activation

Scheme 4. Possible Products of σ-Bond Metathesis between Zr−H of 2m and C−H of Butane

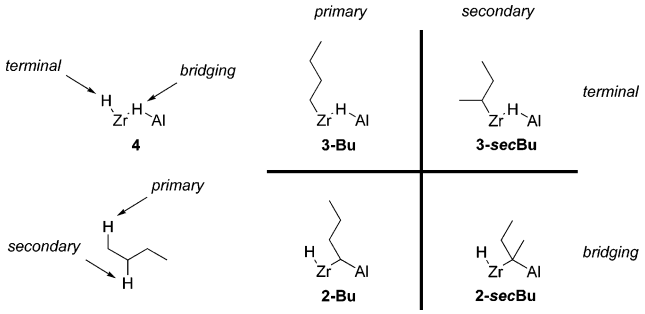

process probably even more favors the formation of **3m-Bu**, so that only pathways involving **3m-Bu** have been further studied. The activation energy leading to **3m-Bu** from **4m** has not been calculated, but is probably close to the activation energy of the reaction **2m-Me** → **1m** (92 kJ·mol^{-1}) because these reactions are very similar.

From a surface alkyl complex like **3m-Bu**, the C−C bond breaking can occur through several reaction pathways: (1) classical β-alkyl transfer (eq 3); (2) nucleophilic substitution at the β-carbon of the alkyl ligand by the hydride (eq 4) with C_β−C_γ breaking, which has already been proposed on a similar silica-supported system;[40] and (3) nucleophilic substitutions at the β-carbon of the alkyl ligand by the hydride with C_α−C_β breaking (eq 5). The α-alkyl transfer (eq 6) giving a carbene and a propyl ligand[41] has been excluded because it would involve an increase of oxidation state, which is not possible for a Zr^{IV} species.

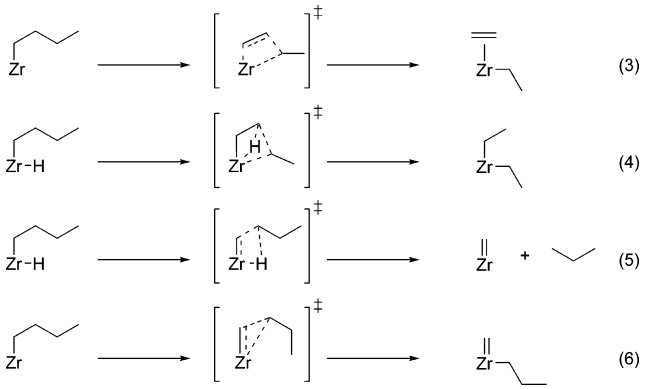

β-Alkyl transfer from the butyl species **3m-Bu** is both highly endoenergetic (ΔE = 129 kJ·mol^{-1}) and highly activated ($\Delta E^{\ddagger}$ = 135 kJ·mol^{-1}), and these values are similar to what has been calculated for silica-supported zirconium hydride.[11,12] Noteworthy, it leads to a coordinated ethylene and an ethyl ligand on Zr, **7m** (Scheme 5). This intermediate has not been obtained for the model of the silica-supported Zr hydride surface complex (neutral),[12] but this slight difference is probably due to the cationic character of the alumina-supported zirconium complex, which further stabilizes the π-olefin complex on the Zr atom.

From **3m-Bu**, the other pathways of carbon−carbon bond cleavage are all even more highly activated: the transition state for the nucleophilic "substitutions" by the hydride at the α- and β-carbons of the butyl ligand of **3m-Bu** (eqs 4 and 5) has an activation energy greater than 250 kJ·mol^{-1} for the former and

(38) Maron, L.; Perrin, L.; Eisenstein, O. *J. Chem. Soc., Dalton Trans.* **2002**, 534−539.
(39) Copéret, C.; Grouiller, A.; Basset, M.; Chermette, H. *ChemPhysChem* **2003**, *4*, 608−611.
(40) Besedin, D. V.; Ustynyuk, L. Y.; Ustynyuk, Y. A.; Lunin, V. V. *Top. Catal.* **2005**, *32*, 47−60.
(41) Chabanas, M.; Vidal, V.; Copéret, C.; Thivolle-Cazat, J.; Basset, J.-M. *Angew. Chem., Int. Ed.* **2000**, *39*, 1962−1965.

Scheme 5. Intermediates in the Hydrogenolysis of Butane after *β*-Alkyl Transfer from 3m-Bu

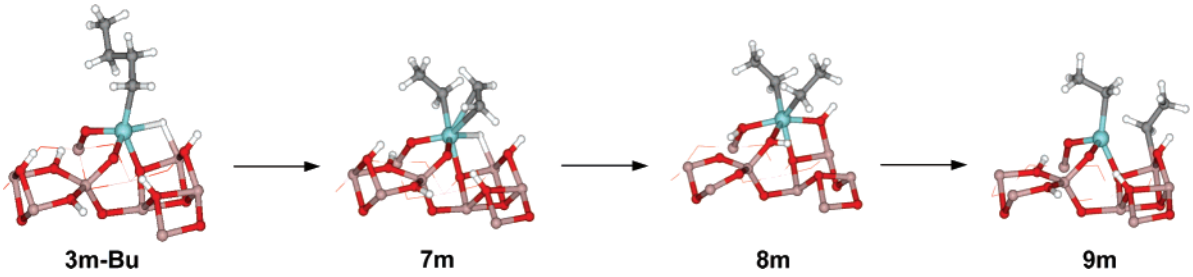

has not been found for the latter, probably because it is even higher in energy. Therefore, the classical β-alkyl transfer giving **7m** is probably the lowest pathway for carbon−carbon cleavage despite its rather high activation energy.

From **7m**, the μ-H migration on ethylene is exoenergetic ($\Delta E = -91$ kJ·mol^{-1}) and gives **8m**, which is stabilized by the migration of a vicinal hydroxyl ligand and of protons ($\Delta E^{\ddagger} = 60$ kJ·mol^{-1}). The reorganization of protons around the other oxygens, which link Zr to the surface, is the result of the high mobility of these protons due to hydrogen bonds.[21] This reorganization is due to the presence of numerous ligands around the zirconium atom. Each ligand is thus less involved in metal−ligand bonds and shares its electron density with neighboring hydrogen atoms, resulting in bridging hydroxyls. The complex **8m** further reorganizes to give **9m**, which is analogous to **1m**, where the methyl ligands are replaced by ethyl ligands (Scheme 5). The liberation of two ethane molecules starting from **9m** to regenerate the catalyst implies the same elementary steps with probably similar activation energies to the formation of the zirconium hydride **2m-Me** starting from **1m**. The whole process starting from **3m-Bu** is exoenergetic ($\Delta E = -15$ kJ·mol^{-1}), and the key elementary step is the β-alkyl transfer, which is the highest energy point on the potential energy surface: it probably corresponds to the rate-determining step.

For the hydrogenolysis pathway involving the activation of the secondary C−H bond of butane via an isobutyl surface intermediate, only the energy of the first alkyl intermediate **3m-*sec*Bu** resulting from the reaction of the terminal hydride of **4m** and the β-alkyl transfer step have been investigated (Figure 3c). In this case, the isobutyl surface complex **3m-*sec*Bu** is 52 kJ·mol^{-1} less stable than **2m** and slightly less stable than **3m-Bu** by 7 kJ·mol^{-1}. The activation barrier leading to **3m-*sec*Bu** is hence probably slightly higher than that leading to **3m-Bu**, i.e., around 100 kJ·mol^{-1}. From **3m-*sec*Bu**, the β-alkyl transfer is also highly endoenergetic and highly activated, although less than that from **3m-Bu**, with ΔE and $\Delta E^{\ddagger}$ of 84 kJ·mol^{-1} and 110 kJ·mol^{-1}, respectively. This illustrates that, in both cases (primary versus secondary C−H activation), the β-alkyl transfer is the key carbon−carbon bond cleavage step, hence the formation of methane, ethane, and propane as primary products and the presence of methane and ethane as final products in the hydrogenolysis of butane.

Conclusion

The theoretical/experimental combined approach applied to the specific case of the characterization of γ-alumina-supported zirconium hydrides shows that the treatment of [$(Al_sO)_2Zr(CH_2tBu)^+(tBuCH_2)Al_s^-$] (**1**) by H_2 yields [$(Al_sO)_2Zr(H)(\mu\text{-}H)Al_{VI}$] (**4**) and [$(Al_sO)_2Zr(H)(\mu\text{-}R)Al_{VI}$] (**2-R**) along with cationic [$(Al_sO)_2Zr(H)]^+$ species in the vicinity of anionic tetrahedral aluminum hydrides [$(Al_{IV}-H)^-$]. Furthermore, during the formation of these hydrides or the hydrogenolysis of alkanes, the alkanes are transformed into their lower homologues to give methane and ethane as the sole final products. The pathway for the hydrogenolysis of alkanes is constituted by two critical steps: C−H activation via σ-bond metathesis and β-alkyl transfer, the subsequent step (i.e., hydrogenolysis of alkyl zirconium intermediates) being exothermic and associated with a low activation barrier. Both critical steps are highly activated (>100 kJ·mol^{-1}), and while the first step (C−H activation) via the butylzirconium species is easier than via the *sec*-butyl zirconium intermediates, it is the reverse for the next step (β-alkyl transfer). This probably explains why this catalyst does not display any selectivity. Notably, the calculated activation energies for alkane hydrogenolysis are of the same order of magnitude as those calculated for the corresponding silica-supported Zr complexes, which is in agreement with the similar observed activity of the two catalysts.

Finally, the identification of the reactants, intermediates, and elementary steps for heterogeneous catalysts including those prepared by surface organometallic chemistry has been a challenge, and here we have shown that modeling can be used as a complementary analytical tool to experimental techniques (IR and NMR spectroscopies). This can lead to a more detailed knowledge of surface species, and further studies are currently underway to exploit these data to develop more efficient catalysts.

OM070145F